Journal of Applied Fluid Mechanics, Vol. 16, No. 7, pp. 1345-1355, 2023.
Available online at www.jafmonline.net, ISSN 1735-3572, EISSN 1735-3645.
https://doi.org/10.47176/jafm.16.07.1692

Experimental Investigation of the Exhaust Device of Turbocharger for Marine Engines

S. Li[†1], Y. Liang[1], X. J. Hou[2], X. L. Yang[3], Y. Q. Wang[4], Y. Q. Zhao[4] and F. L. Zhang[5]

[1]*Liaoning University of Technology, School of Automobile and Traffic Engineering, Jinzhou, Liaoning Province, 121001, China*

[2]*Liaoning University of Technology, School of Civil Engineering, Jinzhou, Liaoning Province, 121001, China*

[3]*Liaoning Technical University, School of Mechanical Engineering, Fuxin, Liaoning Province, 123000, China*

[4]*China North Engine Research Institute, Shanxi Province, 037036, China*

[5]*WEICHAI POWER Co.LTD., Weifang, Shandong Province, 261072, China*

†Corresponding Author Email: lisong_0914@163.com

(Received December 12, 2022; accepted March 1, 2023)

ABSTRACT

In order to reduce the temperature in the marine engine cabin, improve the working environment of the staff and meet the economy and emission requirements, the cooling system of the engine was experimentally investigated in the present study. In this regard, water cooling and air-cooling schemes were studied and the main indicators including engine torque, smoke-emission, and exhaust temperature were analyzed. The obtained results indicate that the highest torque can be obtained from the air-cooling turbine case and air-cooling exhaust pipe. As the applied torque decreases, the outlet smoke first decreases then increases and decreases finally. Moreover, it is found that the water-cooling turbine case and water-cooling exhaust pipe increase the smoke. When the turbocharger is equipped with a water-cooling turbine case and water-cooling exhaust pipe, the higher the engine torque, the higher the turbine exhaust temperature and oil tank temperature, and the greater the reduction of the exhaust temperature. The engine torque is in direct proportion to the fuel consumption. The greater the torque, the higher the engine speed and the greater the fuel consumption. The engine torque is inversely proportional to the fuel consumption rate. The greater the torque, the smaller the fuel consumption rate. In cases with water cooling exhaust devices at 110% loading speed, the temperature after the intercooler is higher than that with the air-cooling exhaust device. After the intercooler, the pressure increases as the applied torque increases, and a higher-pressure ratio can be obtained from the air-cooling exhaust device. The higher the engine torque, the higher the temperature of the turbine exhaust, the higher the outlet temperature of the circulating cooling water, and the higher the temperature in the cabin. It was concluded that the exhaust device of the air-cooling turbine case and water-cooling exhaust pipe can reduce the temperature in the engine parts by up to 2°C, thereby improving the working environment of the cabin staff, economic performance, and the emission index.

Keywords: Turbocharger; Water cooling; Air cooling; Exhaust devices; Engine cabin temperature.

1. INTRODUCTION

With the rapid developments in different industries such as automobile, shipbuilding, aviation, agricultural machinery, and construction machinery, increasingly strict environmental protection regulations have been promoted remarkably. In this regard, the turbocharger has attracted many scholars in diverse industrial fields and has been widely adopted as a standard engine configuration (Zhao and Li 2015). Studies reveal that applying turbocharging technology improves the working performance of the engine, reduces pollutant emissions (Mezher *et al*. 2013), and improves engine efficiency (Su *et al*. 2014). Recently, the turbocharger has developed rapidly as an important auxiliary component of the engine. In this regard, many advances have been made in different fields such as electronics and materials. Accordingly, the turbocharger can be considered as a high-tech product integrating machinery (Zhao *et al*. 2015; Li *et al*. 2021).

Studies show that the ship engine has one of the worst working environments mainly originating from space constraints. For example, once the ship engine fails, the maintenance staff should carry out

maintenance in a confined space with high temperatures and polluted air. In order to improve this challenging working environment, many investigations have been carried out on the cooling and temperature control of the engine. In this regard, Xin (2013) studied the heat dissipation and cooling of diesel engines, applied the first law of thermodynamics to the engine energy balance in the engine, proposed the theory of engine miscellaneous heat loss and heat dissipation, and calculated the cooling performance, cooling capacity and coolant temperature. Fontanesi and Giacopini (2013) applied CFD and FEM methods to investigate engine conjugate heat transfer and thermal loading cycle and fatigue strength, and optimized the water-cooling turbocharger of an internal combustion engine. Moreover, Hansen *et al.* (2013) proposed two methods to control single-phase marine cooling systems based on nonlinear robust control models and then evaluated the performance and robustness of the proposed methods. Accordingly, it was found that both designs have promising robustness to the variation of parameters, while the nonlinear robustness design performs better in terms of noise immunity. Zegenhagen and Ziegler (2015) analyzed the application of an ejector cooling system in a turbocharged gasoline engine to cool the charged air and improve engine efficiency. In order to improve the fuel economy of turbocharged engines under full-loading knock limit operation, Bozza *et al.* (2016) studied the exhaust gas recirculation (EGR) of low-pressure coolant and the water injection into the intake port of the turbocharger. The obtained results showed the introduction of inert gas into the cylinder reduces the tendency of knocking, thereby promoting the combustion performance, while reducing fuel consumption. Further investigations revealed that the heat subtracted by the water evaporation intensifies this effect, thereby improving fuel economy. In this regard, Li *et al.* (2017) and Tornatore *et al.* (2019) demonstrated that cooled EGR can reduce engine soot emissions. Wei *et al.* (2017) found that water injection into the engine cylinder can improve engine performance and reduce NOx and soot emissions. They found that cooling of certain parts of the engine can increase the average effective pressure and efficiency. It was found that the best engine performance can be achieved when fuel is injected with 15% water. Novella *et al.* (2017) studied the intake air cooling of internal combustion engines. They proposed theoretical models, performed experiments, improved the efficiency of the internal combustion engine, and reduced pollutant emissions. Cipollone *et al.* (2013, 2017) proposed a refrigeration unit to cool the engine charge air and found that proper installation of the refrigeration unit inside the intake manifold can provide additional cooling, thereby reducing fuel consumption and significantly reducing pollutant emission. Mohamed *et al.* (2018) integrated the heat discharge during the scavenging cooling process by the exhaust gas in the steam power generation cycle to improve the power generation efficiency of the waste heat recovery system in marine diesel engines. Wu *et al.* (2021) performed numerical simulations and experiments to study the fuel and air systems of diesel engines and analyzed the influence of different thermal management processes on combustion, exhaust temperature, and thermal efficiency. Accordingly, it was found that compared with the fuel strategy, the air system strategy has higher thermal efficiency.

Considering the high temperature of the exhaust gas of the internal combustion engine, the turbocharger bears high heat loads. Consequently, heat dissipation performance greatly affects the service life of the turbocharger (Jiaqiang *et al.* 2016, 2018). In this regard, Lu *et al.* (2021) studied the water-cooled bearing body of turbochargers and analyzed the influence of the flow rate and temperature of cooling water and the surface roughness of the cooling chamber on the cooling performance. Meanwhile, Zhao *et al.* (2018) studied the effect of heat transfer on turbocharger efficiency. Salameh *et al.* (2021) considered the turbine, compressor, and bearing body in the turbocharger as a thermal mass and took the water-cooling bearing body as the thermal barrier between the turbine and compressor. Then they applied a heat transfer model for the analysis. Since no coupling is considered in this method between the compressor and turbine, the calculations and complexity of the problem reduce significantly. Serrano *et al.* (2015) studied the internal convection of small turbochargers using the convective heat transfer coefficient and found that when the applied load is relatively low, the heat loss at the turbine end increases as the enthalpy drops, and all heat transfer is concentrated at the turbine inlet. On the other hand, the heat transfer at the compressor side concentrates at the compressor outlet, which should be considered only under high loads.

Reviewing the literature indicates that most investigations on the turbocharger have focused on the compressor and turbine performance. Moreover, researches on water cooling turbochargers also mainly focus on the heat transfer process from turbine to compressor and the corresponding thermal fatigue. This is especially more pronounced in water cooling bearing bodies. On the other hand, a few investigations have been carried out on the impact of the thermal radiation generated by the turbine case and exhaust pipe on the environment and the working conditions of the staff. The main objective of the present study was to improve the working conditions in a relatively closed space of the marine engine cabin, which is sensitive to the temperature effect caused by the exhaust. In the present study, the water cooling and air-cooling experiments were carried out on a marine engine turbocharger and exhaust pipe to investigate the influence of water-cooling devices, and provide a theoretical basis for future designs.

2. EXPERIMENTAL STUDY

2.1 Determination of the Experimental Scheme

To study the influence of the water-cooling turbine

case and water-cooling exhaust pipe on the engine emission and environment, the water path of the engine is adjusted and three experimental schemes are designed. Table 1 and Fig. 1 show the test cases and test configurations, respectively.

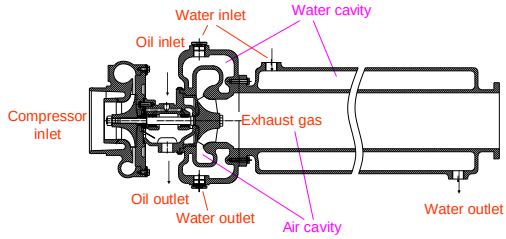

Case 1 Water cooling exhaust pipe and water-cooling turbine case

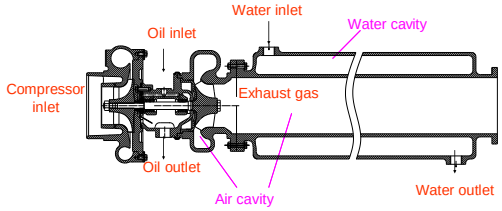

Case 2 Water cooling exhaust pipe and air-cooling turbine case

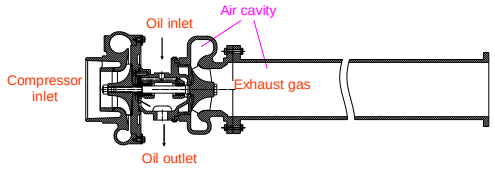

Case 3 Air cooling exhaust pipe and air-cooling turbine case

Fig. 1. Different schemes of the turbocharger.

Table 1 Test cases of the turbocharger and exhaust pipes

Serial No.	Engine status
Case 1	There is circulating water in the exhaust pipe and turbine case (water cooling exhaust pipe and water-cooling turbine case)
Case 2	There is circulating water in the exhaust pipe and no circulating water in the turbine case (water cooling exhaust pipe and air-cooling turbine case)
Case 3	There is no circulating water in the exhaust pipe and turbine case (air cooling exhaust pipe and air cooling turbine case)

Remarks: When the engine is in the three states in Table 1, the loading characteristic test of the rated speed should be carried out according to the rated working conditions (551 kW/1500 rpm) and 110% overloading condition (662 kW/1800 rpm)

2.2 Experimental System

In the present study, experiments were carried out on the engine test bench. Figure 2 indicates that the test bench mainly consists of an engine, turbocharging system, cooling system, dynamometer, and control system, fuel system, lubricating oil system, measurement, and data acquisition system, and pipeline system. The compressed air enters the engine cylinder and adjusts the fuel supply to provide a complete combustion reaction. Then the burned gas enters the turbocharger to promote the turbine to drive the compressor to compress the air, thereby increasing the air density. The pressurized gas enters the engine cylinder after being cooled in the intercooler and then participates in the combustion process. The turbocharger turbine case and exhaust pipes can be mainly divided into water-cooled and air-cooled types. Then the exhaust gas discharged from the turbine is monitored. The experimental setup and the corresponding flow diagram are shown in Fig. 2. Furthermore, the main technical specifications of the diesel engine for the test are shown in Table 2.

Table 2 Technical specifications of the engine

Engine model	12M26
Rated power / speed	551/1500 （kW/rpm）
Overloading power / speed	662/1800（kW/rpm）
Cylinder bore×stroke	150×150 mm
Displacement	31.8 L
Compression ratio	14
Firing sequence	1-8-5-10-3-7-6-11-2-9-4-12
Maximum burst pressure	≤15 MPa
Temperature of diesel engine circulating water outlet	75~85 ℃
Oil temperature	90~95 ℃
Turbine outlet exhaust temperature	≤500 ℃
Oil pressure	400～600 kPa
Exhaust backpressure	≤ 3 kPa
Advance supply angle	27° CA

2.3 Selection of the Turbocharger

During the experiment, H135 turbocharger is used. It is a forward inclined turbocharger with a backward-curved runoff impeller, 7 mainstream blades, and 7 splitter blades. The inlet and outlet diameters of impellers are 86.4 mm and 122 mm, respectively. There is an intake bypass recirculation system with a channel area of 1813 mm2 in the compressor volute. Moreover, the inlet and outlet diameters of the turbine are 106.4 mm and 99.1 mm, respectively. The channel area is 2500 mm^2.

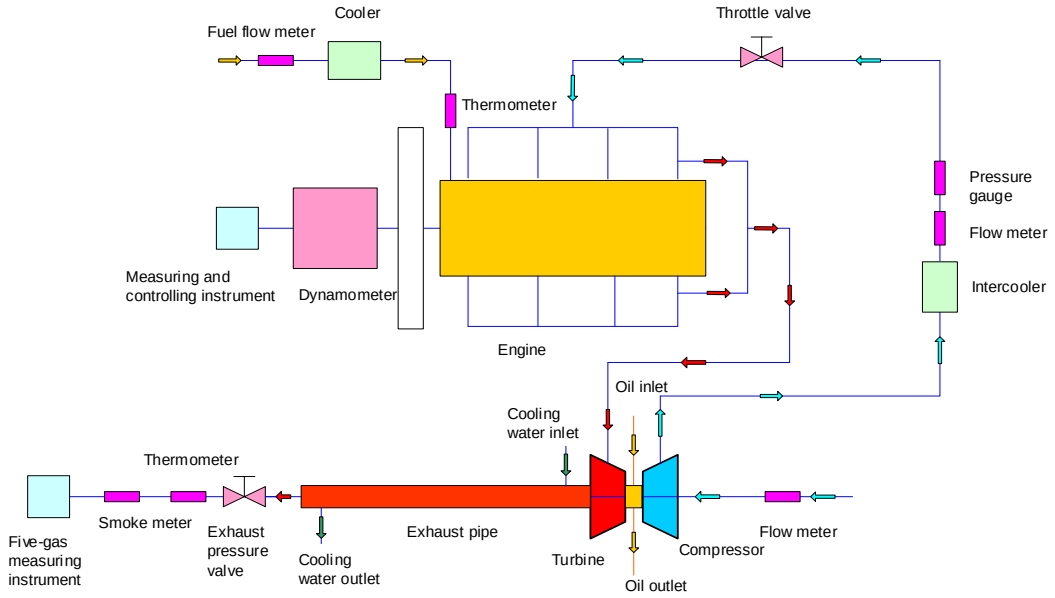

(a) Test schematic diagram and data acquisition point

(b) Test bench

Fig. 2. Engine test bench and data acquisition points.

Table 3 Specifications of measuring instruments in the experiment

No.	Meter	Specifications	Measuring accuracy
1	Hydraulic dynamometer	0-3300 kW	±0.4 FS
2	Engine measuring and controlling instrument	NCK2000	±2%
3	Explosion pressure gauge	0-20 MPa	2.5 grade
4	Pressure gauge	ZBY215-84	±0.5%
5	Thermometer	0-600 ℃	1.6 grade
6	Thermometer	0-200 ℃	1.2 grade
7	Five-gas measuring instrument	FBY-200	±0.3%
8	Smoke meter	FBY-201	±3%
9	Fuel flow meter	SX-GF	±0.5%
10	Turbocharger flow rate	double button flow meter	±1.5%
11	Turbocharger speed	magnetic-electric tachometer	±0.2%

2.4 Experimental Requirements

The test equipment and instruments should be calibrated before the experiment. During the test, the bench air filter with a disposable filter is used. Moreover, light diesel oil (No. 0 according to GB252 standard), and Machine oil (15W/40 CD according to GB11122 standard) with an appropriate antifreeze (Mobil grade) that resists freezing up to -45 ℃ is used. The flow rate of the cooling water is set to 24 m^3/h. During the test, all parameters are measured after the stable running of the diesel engine for 5 min. The test equipment and instruments are shown in Table 3.

The experiment is conducted from a high-power and high-torque operating condition to a low-power and low-torque condition. During the experiment,

several parameters, including ambient pressure and temperature, engine speed, torque, power and smoke, fuel consumption rate, turbine exhaust temperature, oil tank temperature and return temperature of the cooling water, and temperature and pressure of the intercooler exhaust are monitored.

2.5 Experimental Error Processing Method

During the experiment, the effective power of the engine is measured by the bench test. In this regard, the effective torque and crankshaft speed are measured by a dynamometer. Then, the effective power output of the engine through the flywheel is calculated by the following expression:

$$Pe = T_{tq}\frac{2\pi n}{60}\times 10^3 = \frac{T_{tq}n}{9549} \quad (1)$$

where Pe denotes the effective power in kW, T_{tq} is the effective torque in N·m, and n denotes the crankshaft speed in rpm. The fuel consumption rate of the engine can be calculated as follows:

$$be = \frac{B\times 1000\times 9549}{T_{tq}n} = \frac{B\times 1000}{Pe} \quad (2)$$

where be denotes the fuel consumption rate in g/(kW·h，reflecting the fuel consumed by the engine for each kW·h of effective output work. Moreover, B denotes the consumed fuel per hour, kg/h. Uncertainty of the experimental data results can be adopted from the following expression (Moffat R J, 1988):

$$\delta_R = \sqrt{\left(\frac{\partial R}{\partial x_1}\right)^2\delta x_1^2 + \left(\frac{\partial R}{\partial x_2}\right)^2\delta x_2^2 + \cdots + \left(\frac{\partial R}{\partial x_i}\right)^2\delta x_i^2 + \cdots} \quad (3)$$

For the effective power and fuel consumption rate of the engine, uncertainty expression can be rewritten in the form below:

$$\delta_{Pe} = \sqrt{\left(\frac{\partial Pe}{\partial T_{tq}}\right)^2\delta T_{tq}^2 + \left(\frac{\partial Pe}{\partial n}\right)^2\delta n^2} \quad (4)$$

$$\delta_{be} = \sqrt{\left(\frac{\partial be}{\partial B}\right)^2\delta B^2 + \left(\frac{\partial be}{\partial Pe}\right)^2\delta Pe^2}$$

$$= \sqrt{\left(\frac{\partial be}{\partial B}\right)^2\delta B^2 + \left(\frac{\partial be}{\partial T_{tq}}\right)^2\delta T_{tq}^2 + \left(\frac{\partial be}{\partial n}\right)^2\delta n^2} \quad (5)$$

3. Experimental Data Analysis

In the present study, three groups of experiments are carried out on the engine test bench to compare engine smoke, exhaust temperature, fuel consumption, and other indicators under different conditions at the rated speed (1500 rpm) and 110% loading speed (1800 rpm).

3.1 Smoke

Figure 3 shows the relationship between the engine torque and smoke at different operating speeds. The obtained results show that as the applied torque decreases, the smoke decreases first, then increases, and finally decreases once again. Moreover, when the rated speed is 1500 rpm, the torque decreases from 4000 N·M to 1750 N·M. When the torque is 1750 N·M, the smoke is about 0.45 FSN, and then the smoke increases again to about 1400 N·M. Meanwhile, the torque smoke increases to the extreme value, and the smoke is about 0.6 FSN. As the applied torque further decreases, the smoke decreases again.

At a 110% loading speed of 1800 rpm, the torque decreases from 3750 N·M to 2000 N·M, and the smoke decreases. The smoke in the Cases 1 and 2 scheme is about 0.6 FSN, while that in Case 3 scheme is about 0.45 FSN. It is observed that when the applied torque decreases from 2000 N·M to 800 N·M, the smoke increases, reaching the maximum value at 800 N·M. At this time, the smoke varies within the range of 0.85~1.0 FSN. The smoke intensity of Case 3 is the lowest at the rated speed of 1500 rpm, and only at the minimum torque point (360 N·M), it is slightly higher than that of the other two schemes. When the applied torque is less than 3500 N·M, the smoke intensities of Case 1 and

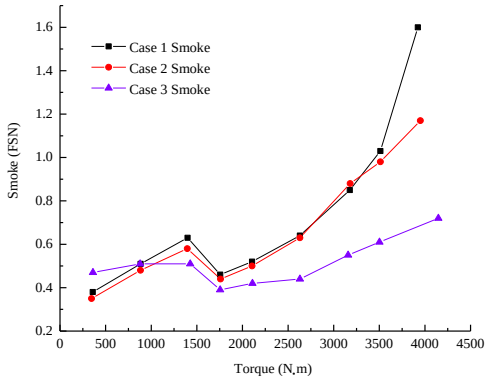

(a) 1500rpm

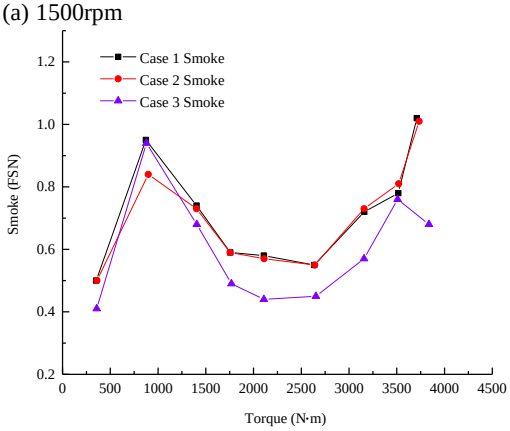

(b) 1800rpm

Fig. 3. Power and smoke at different rated speeds.

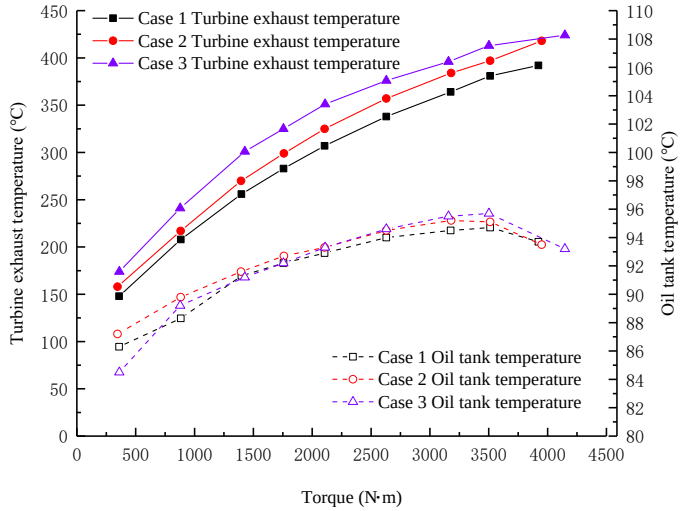

(a) 1500 rpm

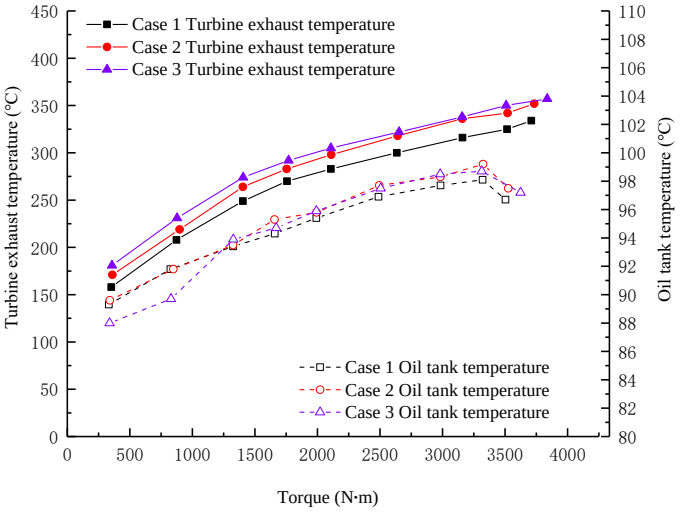

(b) 1800 rpm

Fig. 4. Temperature of the turbine exhaust and oil tank at different rated speeds.

Case 2 are the same. However, when the torque is about 4000 N·M, the smoke intensity of Case 1 is much higher than that of Case 2 and Case 3. Furthermore, at a 110% loading speed of 1800 rpm, smoke intensities of Case 1 and Case 2 are the same and higher than that of Case 3 in the torque range of 3750 N·M to 1400 N·M, while the smoke intensities of Case 1 and Case 3 are the same and higher than that of Case 2 in the torque range of 1400 N·M to 350 N·M. This is because at the loading moment, the fuel supply increases first, while the gas supply is still insufficient. Consequently, the engine torque and the smoke level are high in the initial moments of the experiment. As the engine operates continuously and reaches steady-state conditions after several working cycles, the gas pressure in the exhaust pipe gradually rises, the energy released in the turbine increases, and the turbine speed increases, so the mass of the compressed gas entering the engine cylinder increases, and the smoke level decreases; When the engine operates under the low-torque condition, the air-to-fuel ratio decreases due to the lag of the supercharger response, so the combustion quality deteriorates, thereby increasing the exhaust smoke level, further decreasing the air-to-fuel ratio in the turbocharger, and reducing the operating velocity. Therefore, the smoke level of the engine working at 1800 rpm is higher than that at 1500 rpm when the engine works under low-torque conditions. This may be attributed to the air-cooled exhaust pipe and turbine case in Case 3, while the exhaust pipe and turbine case are water-cooled in Case 1 and Case 2 which increases the heat dissipation. Therefore, the smoke content of Case 1 and Case 2 is higher than that of Case 3.

3.2 Temperatures of the turbine exhaust and the oil tank

Figure 4. shows the relationship between engine torque, turbine exhaust temperature, and oil tank temperature at different working conditions.

It is observed that under the same scheme and the same speed, the greater the applied torque, the higher the turbine exhaust temperature and the higher the oil tank temperature. Moreover, the turbine exhaust temperature of the same scheme at 1800 rpm is lower than that at 1500 rpm, while the

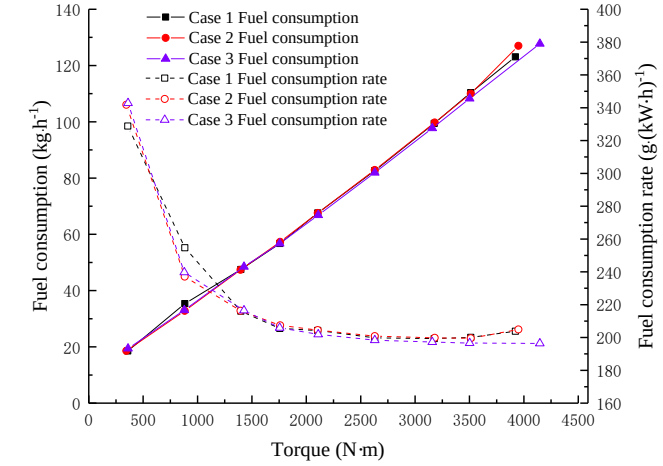

(a) 1500 rpm

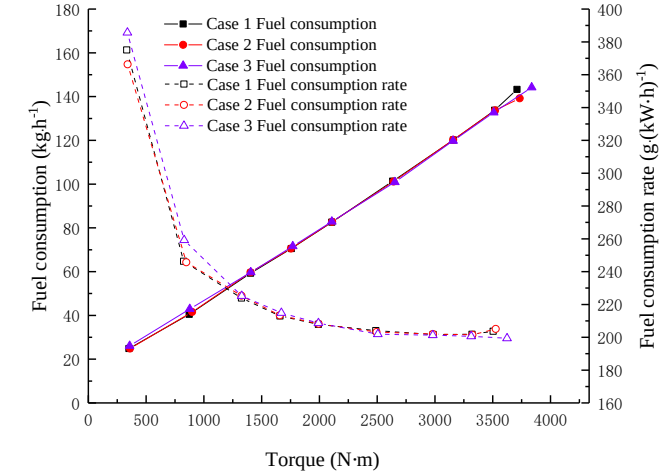

(b) 1800 rpm

Fig. 5. Fuel consumption at different engine speeds.

oil tank temperature is not lower than at 1500 rpm. The obtained results show that the lowest and the highest turbine exhaust temperature are achieved for Case 1 and Case 3, respectively. Under the same working condition, the turbine exhaust temperature in the two schemes is about 30 ℃~50 ℃. The turbine exhaust temperature of Case 2 is between the two, and the cooling efficiency at a low torque is higher than that of high torque. It is observed that the turbocharger is equipped with a water-cooling turbine case and water-cooling exhaust pipe, which can greatly reduce the exhaust temperature.

3.3 Fuel Consumption

Fuel consumption rate is an important index to compare the economy of different engines. In this regard, it is intended to compare the engine performance under three cases in terms of fuel consumption, so the economy of the three cases can also be compared in terms of fuel consumption. Figure 5 shows the relationship between engine torque and fuel consumption and consumption rate at different rated speeds.

It is observed that the engine torque is in direct proportion to the fuel consumption. The higher the applied torque, the higher the fuel consumption. Moreover, the higher the engine speed, the greater the fuel consumption. At the maximum power and torque, the maximum torque can be achieved from Case 3, and the fuel consumption of Case 3 is the same in Case 2 at 1500 rpm and Case 1 at 1800 rpm. Figure 5 indicates that the engine torque is inversely proportional to the fuel consumption rate. The greater the torque, the smaller the fuel consumption rate. When the applied torque varies within the range of 1500 N·M to 4000 N·M, the fuel consumption rate is gentle. When the engine runs at a low torque, the fuel consumption rate increases rapidly.

When the engine torque is set to 750 N·M, the fuel consumption rate in the three schemes changes significantly. At an engine speed of 1500 rpm, the highest fuel consumption rate is achieved from Case 1, where the fuel consumption is about 2.5 kg/h higher and the fuel consumption rate is about 15 g/(kW·h) higher than that of Case 2 and Case 3. When the speed engine is set to 1800 rpm, the highest fuel consumption is obtained from Case 3, where the fuel consumption is about 2 kg/h higher

Table 4 Parameters at maximum power in the loading characteristic test.

Parameters	Case 1		Case 2		Case 3	
	1500 rpm	1800 rpm	1500 rpm	1800 rpm	1500 rpm	1800 rpm
Maximum power/kW	618.4	705.9	620.7	703.5	650.6	723.1
Fuel consumption rate at maximum power/ g/(kW·h)	203.8	203.7	204.9	205.1	196.4	199.4
Smoke at maximum power/FSN	1.60	1.02	1.17	1.01	0.72	0.68
Turbine exhaust temperature at maximum power /℃	392	334	418	352	424	357

and the fuel consumption rate is about 13 g/(kW·h) higher than that of Case 1 and Case 2.

The obtained results from loading characteristic tests at different engine speeds are presented in Figs. 3 and 5, and the comparison is shown in Table 4. It is found that there is a slight difference between the maximum power and the fuel consumption rate at the maximum power of Case 1 and Case 2. Moreover, higher power and lower fuel consumption rate can be achieved from Case 3, indicating that the circulating cooling water removes part of the generated heat. Meanwhile, it is observed that most of the energy loss occurs in the exhaust pipe. The smoke intensity of Case 1 exceeds 1.5 FSN, which is higher than the requirements of China's engineering indicators. The exhaust emission causes serious environmental pollution, but among the studied cases, it has the lowest turbine exhaust temperature. Although the smoke intensity of Case 3 is the lowest, the turbine exhaust temperature is high, resulting in a too high temperature in the engine cabin. The smoke intensity and turbine exhaust temperature of Case 2 is between those of Case 1 and Case 3.

3.4 Temperature and Pressure After the Intercooler

Figure 6 shows the relationship between the engine torque, temperature, and pressure after the intercooler at different engine speeds.

It is observed that at 1500 rpm, the temperature after the intercooler in the three cases is almost 32 ℃. Moreover, when the engine speed increases to 1800 rpm, the after intercooler temperature in Case 1 and Case 2 is almost 36 ℃, while the after intercooler temperature in Case 3 varies between 29 ℃ and 33 ℃, and it increases as the applied torque increases. It is found that the after intercooler pressure in the studied cases increases as the applied torque increases. The after intercooler pressure in Case 1 and Case 2 are close to each other, and the highest after intercooler pressure is achieved from Case 3, indicating that the compressor pressure ratio in Case 3 is the highest.

3.5 Temperature of Circulating Cooling Water at the Pipe Outlet

Figure 7 shows the relationship between engine torque and temperature of circulating cooling water at pipe outlet at different engine speeds. It is observed that the turbocharger speed has a slight effect on the temperature of the circulating cooling water at the pipe outlet. Generally, the greater the engine torque, the higher the turbine exhaust temperature and the higher the outlet water temperature of the circulating cooling water. Temperatures of the circulating cooling water at the pipe outlet in Case 1 and Case 2 are close, and both are higher than that of Case 3, indicating that the dissipated heats by the circulating cooling water of Case 1 and Case 2 are almost the same, while the heat dissipation is relatively low in Case 3. Consequently, the highest turbocharger efficiency and pressure ratio and the lowest fuel consumption rate can be achieved from Case 3.

3.6 Temperature in the Engine Cabin

In order to cool the engine cabin, two fans are used for ventilation. The rated power and flow rate of the fans are 2.2 kW and 9000 m3/h, respectively. Fiure. 8 shows the temperature distribution in the engine cabin of the three studied cases. It is observed that the temperature in the cabin increases as the applied engine torque increases. When the engine speed is set to 1500 rpm, the cabin temperature is relatively higher than that at 1800 rpm. Moreover, as the engine torque increases, the temperature difference between the two speeds increases. Among the three cases, the lowest temperature in the engine cabin can be achieved from Case 1. At an engine speed of 1500 rpm, the temperature in the engine cabin varies within the range of 35.2 ℃~ 45.3℃, while such variation at 1800 rpm is in the range 35.5℃ ~ 41.1℃. For Case 2 and an engine speed of 1500 rpm and 1800 rpm, variation of the temperature range in the engine cabin is in the range 35.4℃~ 46.3℃ and 35.9℃~ 43.1℃, respectively. The highest temperature in the engine cabin is achieved from Case 3, where the variation range of the engine cabin at 1500 rpm and 1800 rpm, is 36.1℃~ 47.9℃ and 36.2℃~ 43.2℃, respectively. At 1500 rpm, the temperature difference between Case 1 and Case 3 subjected to a torque of 2105 N·M is 3.2℃. When the applied torque reaches 2630 N·M, the temperature difference between the two cases is maximized and reaches 3.4℃. Moreover, when the torque approaches 2630 N·M, the temperature difference between Case 1 and Case 2 is the largest and approaches 2 ℃.

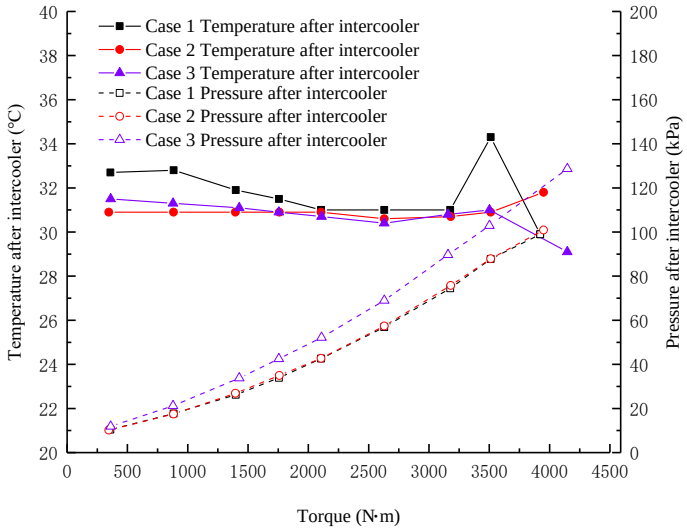

(a) 1500 rpm

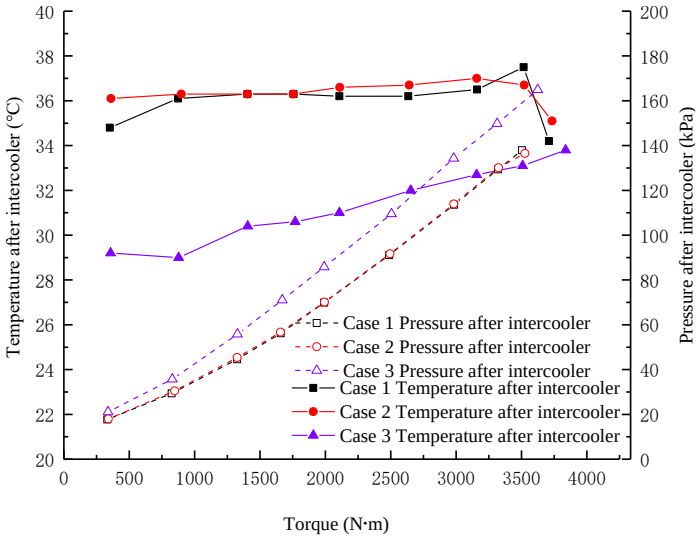

(b) 1800 rpm

Fig. 6. Temperature and pressure after intercooler at different engine speeds.

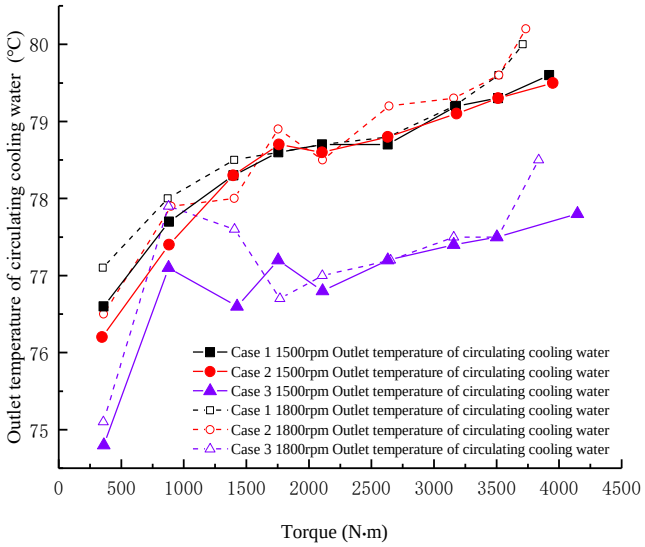

Fig. 7. Outlet temperature of the circulating cooling water at different engine speeds.

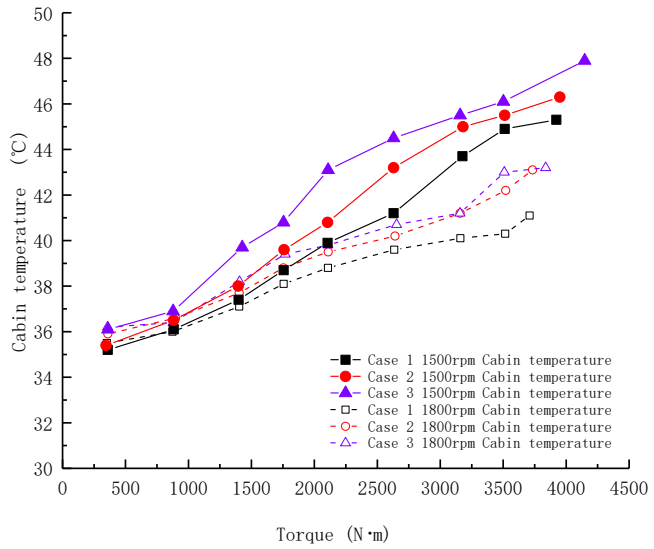

Fig. 8. Distribution of the temperature in the engine cabin at different engine speeds.

In order to reduce the temperature in the engine cabin and improve the working environment of the staff, three cases are considered in the present study, and different indicators such as engine power, exhaust smoke, and fuel consumption are considered in this regard. The obtained results demonstrate that the highest performance of the exhaust device can be achieved from Case 2.

4. CONCLUSION

In the present study, the water cooling and air-cooling exhaust devices of the turbocharger were studied. Based on the obtained results, main achievements can be summarized as follows:

(1) As the applied torque decreases, the smoke first decreases then increases, and decreases finally. The water-cooling turbine case and exhaust pipe will increase the smoke. At the same speed, the greater the engine torque, the higher the turbine exhaust temperature and oil tank temperature. The water-cooling turbine case and water-cooling exhaust pipe in the turbocharger greatly reduce the exhaust temperature.

(2) The engine torque is in direct proportion to the fuel consumption. The greater the applied torque, the greater the fuel consumption. Meanwhile, the higher the engine speed, the greater the fuel consumption. The engine torque is inversely proportional to the fuel consumption rate. The greater the applied torque, the smaller the fuel consumption rate.

(3) At the rated speed, temperatures of the studied cases after the intercooler are close. However, at 110% loading speed, temperatures of Case 1 and Case 2 after intercooler with water cooling exhaust device are close and higher than that in the turbocharger with an air-cooling exhaust device. After the intercooler, the pressure increases as the applied torque increases, and a higher-pressure ratio can be obtained from the air cooling exhaust device.

(4) The turbocharger speed has a negligible effect on the outlet temperature of circulating cooling water. The higher the engine torque, the higher the turbine exhaust temperature, the higher the outlet temperature of the circulating cooling water. Moreover, the temperature in the engine cabin increases.

Based on the performed analyses, parameters of the exhaust device of air-cooled turbine and water cooled exhaust pipe can be optimized to reduce the temperature in the engine parts by up to 2℃, thereby improving economic performance of the engine, improving the working environment of the staff, reducing emission indicators.

ACKNOWLEDGEMENTS

The authors appreciate the Liaoning Provincial Department of Education Project under Grant LJKZ0367.

CONTRIBUTORS

S. Li designed the research. Y.Q. Wang, Y.Q. Zhao and F.L. Zhang processed the corresponding data. S. Li and Y. Liang wrote the first draft of the manuscript. X.J. Hou and X.L. Yang helped to organize the manuscript.

CONFLICT OF INTEREST

S. Li, Y. Liang, X. J. Hou, X. L. Yang, Y. Q. Wang, Y. Q. Zhao and F. L. Zhang declare that they have no conflict of interest.

REFERENCES

Bozza, F., V. D. Bellis and L. Teodosio (2016). Potentials of cooled egr and water injection for knock resistance and fuel consumption improvements of gasoline engines. *Applied*

Energy 169, 112-125.

Cipollone, R., D. D. Battista and D. Vittorini (2017). Experimental assessment of engine charge air cooling by a refrigeration unit. *Energy Procedia* 126, 1067-1074.

Fontanesi, S and Giacopini M (2013). Multiphase CFD–CHT optimization of the cooling jacket and FEM analysis of the engine head of a V6 diesel engine. *Applied Thermal Engineering* 52.2, 293-303.

Hansen, M., J. Stoustrup and J. D. Bendtsen (2013). Modeling and control of a single-phase marine cooling system. *Control Engineering Practice* 21.12, 1726-1734.

Jiaqiang, E., M. Liu, Y. W. Deng, H. Zhu and J. K. Gong (2016). Influence analysis of monolith structure on regeneration temperature in the process of microwave regeneration in diesel particulate filter. *Canadian Journal of Chemical Engineering* 94, 168-174.

Jiaqiang, E., Z. Zhang, Z. Tu, W. Zuo, W. Hu, D. Han and Y. Jin (2018). Effect analysis on flow and boiling heat transfer performance of cooling water-jacket of bearing in the gasoline engine turbocharger. *Applied Thermal Engineering* 130, 754-766.

Li, S., X. Yang, W. Li and M. Tang (2021). Investigating the influence of the inlet bypass recirculation system on the compressor performance. *Journal of Applied Fluid Mechanics* 14(5), 1295-1305.

Li, T., T. Yin and B. Wang (2017). Anatomy of the cooled EGR effects on soot emission reduction in boosted spark-ignited direct-injection engines. *Applied Energy* 190, 43-56.

Lu, C., J. Li and D. Tan (2021). Analysis on the influence mechanism of cooling water on turbocharger and optimum coolant mass flow rate intelligent prediction. *Mathematical Problems in Engineering* 1-14.

Mezher, H., D. Chalet, J. Migaud and P. Chesse (2013). The application of a wave action design technique with minimal cost on a turbocharged engine equipped with water cooled charge air cooler aimed for energy management. *Energy Procedia* 36.1, 948-957.

Moffat, R. J. (1988). Describing the uncertainties in experimental results. *Experimental Thermal and Fluid Scienc* 1, 3-17.

Mohamed, T. M., A. T. Mohamed, M. E. M. Wael and I. S. Ali (2018). Utilizing the scavenge air cooling in improving the performance of marine diesel engine waste heat recovery systems- ScienceDirect. *Energy* 142, 264-276.

Novella, R., V. Dolz, J. Martín and L. Royo-Pascual (2017). Thermodynamic analysis of an absorption refrigeration system used to cool down the intake air in an internal combustion engine. *Applied Thermal Engineering* 111, 257-270.

Salameh, G., G. Goumy and P. Chesse (2021). Water cooled turbocharger heat transfer model initialization: Turbine and compressor quasi-adiabatic maps generation. *Applied Thermal Engineering* 185, 116430.

Serrano, J. R., P. Olmeda, F. J. Arnau, M. A. Reyes-Belmonte and H. Tartoussi (2015) A stu+-dy on the internal convection in small turbochargers. Proposal of heat transfer convective coefficients. *Applied Thermal Engineering* 89: 587-599.

Su, J., X. Min, T. Li, G. Yi and J. Wang (2014). Combined effects of cooled EGR and a higher geometric compression ratio on thermal efficiency improvement of a downsized boosted spark-ignition direct-injection engine. *Energy Conversion & Management* 78, 65-73.

Tornatore, C., F. Bozza, V. Bellis De, L. Teodosio, G. Valentino and L. Marchitto (2019). Experimental and numerical study on the influence of cooled EGR on knock tendency, performance and emissions of a downsized spark-ignition engine. *Energy* 172, 968-976.

Wei, M., N. T. Sa, R. F. Turkson, J. Liu and G. Guo (2017). Water injection for higher engine performance and lower emissions. *Journal of the Energy Institute* 1-15.

Wu, B., Z. Jia, Z Li, G. Liu and X. Zhong (2021). Different exhaust temperature management technologies for heavy-duty diesel engines with regard to thermal efficiency. *Applied Thermal Engineering* 186, 116495

Xin, Q. (2013). Diesel engine heat rejection and cooling. *Diesel Engine System Design* 825-859.

Zegenhagen, M. T. and F. Ziegler (2015) Feasibility analysis of an exhaust gas waste heat driven jet-ejector cooling system for charge air cooling of turbocharged gasoline engines. *Applied Energy* 160, 221-230.

Zhao, D. and L. Li (2015). Effect of choked outlet on transient energy growth analysis of a thermoacoustic system. *Applied Energy* 160, 502-510.

Zhao, D., E. Gutmark and P. Goey De (2018). A review of cavitybased trapped vortex, ultra-compact, high-g, inter-turbine combustors. *Progress in Energy and Combustion Science* 66, 42-82.

Zhao, D., C. Ji, X. Li and S. Li (2015). Mitigation of premixed flame-sustained thermoacoustic oscillations using an electrical heater. *International Journal of Heat and Mass Transfer* 86, 309-318.